PEGylated Viral Nanoparticles for Biomedicine: The Impact of PEG Chain Length on VNP Cell Interactions In Vitro and Ex Vivo

ARTICLE *in* BIOMACROMOLECULES · APRIL 2009

Impact Factor: 5.75 · DOI: 10.1021/bm8012742 · Source: PubMed

2 AUTHORS:

Nicole F Steinmetz
Case Western Reserve University
79 PUBLICATIONS **1,596** CITATIONS
SEE PROFILE

Marianne Manchester
University of California, San Diego
95 PUBLICATIONS **4,785** CITATIONS
SEE PROFILE

Published in final edited form as:
Biomacromolecules. 2009 April 13; 10(4): 784–792. doi:10.1021/bm8012742.

PEGylated Viral Nanoparticles (VNPs) for Biomedicine: the Impact of PEG Chain Length on VNP cell interactions *in vitro* and *ex vivo*

Nicole F. Steinmetz and **Marianne Manchester***
Department of Cell Biology, Center for Integrative Molecular Biosciences, The Scripps Research Institute, La Jolla, California, 92037, USA

Abstract

PEGylation is an effective strategy for reducing biospecific interactions for pharmaceuticals. The plant virus *Cowpea mosaic virus* (CPMV) has been studied for potential nanobiomedical applications by virtue of its natural interactions with mammalian endothelial cells. To investigate the degree of PEGylation required to retarget CPMV-based formulations to other destinations, two CPMV-PEG formulations, CPMV-PEG1000 (P1) and CPMV-PEG2000 (P2) were tested. Modeling suggested that the PEG chains were displayed as flattened mushrooms on the particle with an estimated surface grafting area of 0.53 % for P1 and 0.83 % for P2. Only the P2 formulation effectively shielded the particles from interacting with cells or tissues, suggesting that either key interacting regions on the particle surface were blocked, or that a sufficient hydration shell had been generated to inhibit cellular interactions. The large CPMV surface area available after PEGylation allows further attachment of imaging and therapeutic molecules to the particle to generate multifunctionality.

Keywords

Viral nanoparticles; *Cowpea mosaic virus*; PEGylation; Nanotechnology; Biomedicine

Introduction

The conjugation of polyethelyene glycol (PEG) chains to proteins or nanomaterials, termed PEGylation, is increasingly being used for pharmaceuticals and other biomedical applications. PEGylation allows the efficient reduction or blocking of biospecific interactions between proteins or nanomaterials and cells or tissues. PEG is a neutrally charged, highly hydrophilic polymer that is non-toxic (demonstrated for PEG with a molecular weight ≥1000 Da) and FDA-approved. PEGylation of pharmaceuticals, such as liposomes, therapeutic proteins, dendrimers, and other nanomaterials, is an effective strategy to increase water solubility and stability of the materials, as well as to improve pharmacokinetics, reduce renal clearance, and reduce immunogenicity [1–3].

Our goal is to design multifunctional and targeted nanodevices for imaging and drug delivery systems using the well characterized plant virus *Cowpea mosaic virus* (CPMV). CPMV particles are monodisperse with a diameter of approximately 30 nm, have a high degree of symmetry and polyvalency, are extremely stable to pH, temperature and solvents, can be quickly and inexpensively produced in gram quantities, are biocompatible and non-infectious for humans, and show *in vivo* bioavailability. Last but not least, CPMV presents a tunable and

CORRESPONDING AUTHOR FOOTNOTE: Marianne Manchester, PhD, Department of Cell Biology, Center for Integrative Molecular Biosciences, The Scripps Research Institute, La Jolla, California, 92037, USA, Fax: (+1) 858 784 7979, E-mail: marim@scripps.edu.

programmable nanomaterial, because the particles can be modified by genetic manipulation or chemical conjugation (reviewed in 4).

The potential of CPMV as a tool for biomedical applications has also been demonstrated. Fluorescently labeled CPMV probes effectively visualize the vasculature *in vivo* [5]. It was found that fluorescent CPMV binds to and is internalized by endothelial cells *in vivo*. Interaction of CPMV with mammalian cells is mediated via 54 kDa, non-glycosylated cell surface protein[5,6].

In order to develop "smart" targeted tools for imaging or drug-delivery using CPMV as a platform, one must overcome the natural interactions of CPMV with the mammalian vasculature. Previous studies have shown that PEGylating CPMV is an effective strategy to avoid CPMV-cell surface interactions[5,7,8]. This is holds true for other VNPs, for example, interaction of *Tobacco mosaic virus* with cells can also be inhibited by PEGylation9,[10]. In the case of CPMV, it was found that administration of CPMV particles displaying around 30 copies of PEG5000 (i.e. PEG of a molecular weight of 5000 Da) per virion effectively shielded the particles from inducing a primary immune response [8]. Further, CPMV nanoparticles decorated with 30 copies of PEG3400 did not interact with mammalian vasculature *in vivo* [5]. Also, a CPMV formulation decorated with 60 copies of PEG500 blocked interactions with tumor cells *in vitro* [7].

Overall, the aforementioned studies are in good agreement and show that PEGylation of CPMV results in the desired shielding effect. However, attempts to compare the blocking efficiency of different formulations, i.e. PEG length and PEG density, have not been carried out. In general, effectiveness of a PEGylation strategy depends upon the number of PEGs attached, the molecular weight of the PEG used, its structure and conformation, and location of attachment site [2]. These factors influence the conformation of the PEG polymer and hence the surface grafting area, i.e. the area that is effectively shielded. When designing materials for imaging or targeted drug-delivery, the fewer PEG moieties attached – while still achieving shielding effect – the better. The fewer PEG chains attached, the more free attachment sites remain available on the material for further modification, such as the attachment of imaging or therapeutic molecules.

In order to develop multifunctional CPMV-based nanoparticles it is important to understand the general design principles of PEGylating CPMV that would provide the minimal grafting area while still providing shielding and allowing attachment of additional molecules. To this end we compared two different CPMV-PEG formulations, where PEG1000 or PEG2000 were coupled to solvent-exposed Lys residues on CPMV. CPMV Lys reactivity has been extensively studied and the atomic coordinates and the position of the reactive Lys residues on the capsid surface are known11,12. Both PEG1000 and PEG2000 are commercially available as activated succinimide esters allowing for straightforward bioconjugation. Further, these two polymers are expected to be safe and should not lead to solubility problems upon storage. Cytotoxicity has been reported for lower molecular weight PEG chains ($\leq$ 4 1000 Da)[2]. In contrast, higher molecular weight PEG moieties ($\geq$ 3400 Da) can lead to aggregation or precipitation of the particles upon storage. The latter is not surprising considering the fact that higher molecular weight PEGs are commonly used to concentrate and purify virus particles including CPMV.

We specifically addressed the question whether CPMV particles displaying PEG1000 versus PEG2000 can be used to effectively inhibit interaction of CPMV with cells *in vitro* and tumor tissues *ex vivo*, and whether one or the other formulation is more effective in blocking CPMV-cell interactions. The number of PEG molecules attached to CPMV was quantified, and the particle properties such as particle size and conformation of presented PEG chains on the particle surface were analyzed. This was performed using gel electrophoresis, double-labeling

strategies with fluorescent dyes, size exclusion chromatography (SEC), transmission electron microscopy (TEM), and dynamic light scattering (DLS). Next, the biological properties and the efficiency in blocking or reducing interaction of CPMV with human cells and tissues were analyzed using flow cytometry and confocal microscopy.

Materials and Methods

Propagation of CPMV

Propagation and purification of CPMV was performed by standard procedures [13]. The concentration of purified virions was determined photometrically at a wavelength of 260 nm using the molar extinction coefficient of $\varepsilon = 8.1$ mL mg^{-1} cm^{-1}.

Chemical bioconjugation of PEG and AlexaFluor647 to CPMV

PEG and AlexaFluor molecules were covalently attached to solvent exposed Lys residues on CPMV using succinimide activated esters. PEG succinimidyl ester with a molecular weight of 1000 Da and 2000 Da were purchased from NANOCS, New York. AlexaFluor647 succinimidyl ester was purchased from Invitrogen, Carlsbad. For bioconjugation PEG or AlexaFluor647 was dissolved in DMSO, the labels were used in a molar excess of 3000 to CPMV (2–3 mg mL^{-1}), the reaction was carried out overnight at room temperature (in the dark when working with the fluorescent dye) in a PBS:DMSO mixture of 8:2. Samples were purified using gradient ultracentrifugation in 10–40 % sucrose gradients in 0.1 M phosphate buffer pH 7.0 (Beckman SW 28 Ti rotor, 28700 rpm, 3 hrs, 4 °C) followed by ultrapelleting (Beckman 50.2 Ti rotor, 42000 rpm, 3 hrs, 4 °C). CPMV was re-suspended in PBS and stored at 4 °C.

Native and Denaturing Protein Gel Electrophoresis of PEGylated CPMV particles

20 μg of CPMV, P1, and P2 in PBS (in loading dye, MBI Fermentas) were analyzed on 1.2 % (w/v) agarose gels in 1x TBE buffer, running buffer was 0.5x TBE. Protein subunits were analyzed on denaturing 4–12 % NuPage gels (Invitrogen) using 1× MOPS buffer. 20 μg of CPMV, P1, and P2 in PBS (added LDS loading buffer; Invitrogen) were analyzed. After completion of the electrophoretic separation the particles and protein subunits, respectively, were stained using Coomassie Blue. Photographs of the gels were taken using FluorChemSP imaging system.

Size Exclusion Chromatography (SEC) of PEGylated CPMV particles

CPMV, P1, and P2 particles were analysed on a Superdex200 column using the AKTA Explorer. 500 μl of 0.1 mg mL^{-1} concentrated samples in PBS were analyzed at a flow rate of 0.5 mg mL^{-1}.

Transmission Electron Microscopy (TEM) of PEGylated CPMV particles

7.5 μl 0.1 mg mL^{-1} CPMV, P1, and P2 in PBS were added onto carbon coated copper grids (400 mesh, Agar Scientific). An equal volume 2 % (w/v) uranyl acetate was added for negative staining (1 min at room temperature). The grids were dried using filter paper and imaged using a Phillips CM100 electron microscope.

Quantification of PEG labels per CPMV particle

PEG labels per subunit were quanatified by comparing the protein band intensity in denaturing protein gels after Coomassie staining using FluorChemSP software. Five samples each (P1 and P2) were analyzed. Statistical analysis of differences between S of P1 and P2 and L of P1 and P2 was performed using Student 2-tailed T-test (Microsoft Excel). Alternatively, labels were quantified using a double-labeling strategy. Particles were first labeled with PEG1000 and PEG2000, respectively, and then with AlexaFluor647. Dyes were quantified using UV/visible

spectroscopy and the specific extinction coefficient for the AlexaFluor dye 647 (ε = 20300 M^{-1} cm^{-1}).

Dynamic light scattering (DLS) of PEGylated CPMV particles

CPMV, P1, and P2 at a concentration of 0.1 mg mL^{-1} in PBS were filtered through 0.2 micron filters prior to analysis using a DynaPro Plate Reader (Wyatt) and Dynamics software.

In Vitro Binding Studies using PEGylated CPMV and HT-29 cells

HT-29 cells were grown in RPMI medium (Invitrgogen, Carlsbad) added 10 % fetal bovine serum and 1 % glutamine and 1 % penstrep. Cells were collected using Enzyme-free Hank's based Cell Dissociation Buffer (Gibco) and distributed in 200 μl portions at a concentration of 5×106 cells/ml in 96-well V-bottom shaped plates. For binding assays, prior to adding CPMV, P1, or P2, cells were fixed with 2 % (v/v) formaldehyde in PBS for 20 min at room temperature. Different virus formulations were added using 1×10^5 virus particles per cell and incubated at 4 °C for 60 min. For uptake studies virus particles were added to live cells and incubated at 37 °C for 60 min prior to fixing the cells. Staining was achieved using a polyclonal anti-CPMV antibody followed by a goat anti-rabbit secondary antibody conjugated to AlexaFluor647. All steps were carried out at 4 °C, in between each step cells were washed three with PBS buffer containing 1 mM EDTA pH 8.0, 25 mM HEPES pH 7.5 and 1 % fetal bovine serum. Cells were re-suspended and analyzed using a FACS Calibur instrument (BD Biosciences, Franklin Lakes, NJ). At least 10,000 events, that were gated for single and live cells, were collected. Experiments were repeated at least twice, and within each experiment three replicates of each sample were measured and data analyzed using FlowJo 8.6.3 software (Tree Star, Inc, Ashland, OR).

Ex Vivo Binding Studies using PEGylated CPMV and HT-29 tumor sections

Tumors were generated in athymic nude mice (Nude/WEHI, Scripps Rodent Breeding Colony) using the human colon carcinoma cell line HT-29. Studies were performed in accordance with protocols approved by the Scripps Research Institutional Animal Care and Use Committee (IACUC). Cells were mixed 1:1 vol/vol with Matrigel (BD Biosciences, Franklin Lakes, NJ) and 1×10^6 cells were injected bilaterally and subcutaneously in the flank. After three weeks of growth, animals were euthanized and tumors were excised and embedded in OCT medium (Tissue Tek). Frozen sections (10 μm) were prepared on a Leica cryomicrotome, collected on slides and stored at −20 °C. Tumor sections were fixed in iced cold 95 % ethanol for 20 min, and then blocked using 10 % goat serum in PBS for 60 min at room temperature. 10 μg of each virus formulation (CPMV, P1, and P2) were added to the sections for 60 min at room temperature. Polyclonal anti-CPMV antibody was added to the cells in 5 % goat serum in PBS followed by secondary goat anti-rabbit AlexaFluor555-labeled antibody, each antibody was incubated for 60 min at room temperature. Cell nuclei were stained by adding 4',6-diamidino-2-phenylindole (DAPI). In between each step the slides were rinsed three times with PBS. Slides were mounted using Vecta Shield mounting medium (Vector Laboratories). Sections were imaged using a Biorad 2100 confocal microscope with a 40x oil objective. Data were analyzed and images were created using ImageJ.

Results and Discussion

PEG conjugation to CPMV

To covalently decorate CPMV with PEG polymers, *N*-hydroxysuccinimide-activated PEG1000 or PEG2000 conjugates were coupled to solvent-exposed Lys residues on CPMV to yield P1 and P2 formulations, respectively. P1 and P2 were found to be intact and stable upon storage in buffer at pH 7.0–7.2 at 4 °C for at least six months, as indicated by native and

denaturing gel electrophoresis, SEC, and TEM (Figure 1). In addition, double-labeling techniques (see below) also yielded intact and stable particles, indicating that at least as determined by these methods PEGylated CPMV particles are structurally as sound as native CPMV particles.

Native gel electrophoresis of P1 and P2 particles indicated that the particles were intact and that PEG chains were indeed attached (Figure 1A). PEGylated samples migrated slightly slower compared to native CPMV particles, and this effect was more apparent for the P2 formulation (Figure 1A, lane 3). The mobility of CPMV in native gels is influenced by various factors including charge and size [14]. PEG is a non-charged polymer, however, it is attached to Lys residues, which contribute to the overall surface charge of CPMV. The attachment of small non-charged molecules to Lys side chains equates to a reduction in positive charge, thus making the particles more negatively charged and leading to increased mobility of the virions in the gel matrix (see for example Fig 1A, lane 4: CPMV-fluorescent dye conjugate). The fact that the migration of PEGylated particles is slightly retarded in the gel compared to native CPMV can be explained by the PEG moieties being presented as flexible chains and thus inhibiting migration. An increased hydrodynamic radius of the particles could also lead to the observed pattern. In summary the band pattern suggests successful attachment of the PEG moieties to CPMV. Intact CPMV particles result in two distinct bands on native agarose gels, this phenomenon can be explained by the different electrophorectic forms of S derived from a proteolytic cleavage process that occurs during replication *in planta* [14]. The fact that chemically modified CPMV particles appear as one band, or not as two distinct bands, may be explained by an increased polydispersity introduced through PEGylation.

Denaturing protein gels then confirmed covalent attachment of PEG polymers to both, the small (S) and large (L) coat protein subunit of CPMV (Figure 1B). CPMV consist of 60 identical copies of each of the S and L subunits [15]. We found that PEG moieties were attached to both subunits, however not every subunit was labeled, as native and modified S and L both were detected on protein gels (Figure 1B).

SEC and TEM further confirmed the integrity of P1 and P2 particles. The ratio of the absorbance peak at 260 nm (derived from the encapsidated RNA molecules) to the absorbance peak at 280 nm (derived from the protein coat) of P1 and P2 formulations, as determined by SEC, were in good agreement with data typically obtained for intact CPMV particles, giving a A260nm:A280nm ratio of ≈ 1.8 and thus indicating that the particles were indeed intact (Figure 1C). Interestingly, the elution times vary from particle to particle formulation: native CPMV elutes at 25.7 min, P1 elutes at 24.3 min, and P2 elutes at 23.7 min. This is in good agreement with the particles being PEGylated, as the shorter elution times of the P1 and P2 formulation *versus* native CPMV indicate an increased molecular weight. Differences between P1 and P2 can be explained by P2 being decorated with the higher molecular weight PEG.

Using TEM imaging, monodisperse intact particles with a diameter of approximately 30 nm were observed, further confirming intactness of the PEGylated particles (Figure 1D). P1 and P2 particles appeared to be slightly different compared to native CPMV. The surface of the icosahedral particles appeared altered and slightly more irregular; this is more apparent for the P2 formulation.

Interestingly, an unusually high amount of internally stained PEGylated CPMV particles was observed, again this effect was more strongly observed for P2 compared to P1 particles. The uranyl acetate negative stain can diffuse into the particles but typically stains only the interior of empty virions that lack RNA molecules. We can exclude a high number of empty particles being present in the P1 and P2 population based on the absorbance ratio of A260nm:A280nm, and by ethidium bromide-staining of the particles following native gel electrophoresis that

confirms the presence of nucleic acid (not shown). PEGylation may alter the surface properties of the P1 and P2 in that way that allows uranyl acetate to diffuse into RNA-containing CPMV particles, either by modifying the chemical nature of the surface or the porosity of the virus capsid. This phenomenon has also been observed with CPMV-oligonucleotide complexes (Steinmetz, unpublished). One potential explanation is that upon attachment of those polymers structural re-arrangements and conformational changes occur which may introduce holes or pores into the structure, thus allowing uranyl acetate to diffuse into RNA-containing particles. Another possibility is that the PEGylated CPMV particle is also more highly hydrated, and the water adlayer may influence binding of uranyl acetate such that more of the negative stain accumulates within the particles. In summary the data indicate that PEG1000 and PEG2000 polymers were successfully attached to CPMV particles.

Biochemical and Biophysical Properties of P1 and P2

To quantify the number of PEG molecules per CPMV, two independent methods were used. First, the number of labels per subunit was quantified by comparing the protein band intensity in denaturing protein gels after Coomassie staining. Using this method we found that an average of 22 ± 1 PEG1000 chains were attached to the P1 formulation and an average of 27 ± 4 labels were found per P2 formulation (Figure 2A). The distribution of labels was not evenly split between S and L subunits; in both cases more PEGs were attached to L. Differences between P1 and P2 were not large, but were statistically significant. To date it has been proven difficult to precisely quantify the number of PEG labels per protein formulation. Direct staining methods, such as barium iodide staining [16], have been developed. However, this method lacks sensitivity, and was found to be not applicable for PEGylated CPMV samples (not shown). Quantitation of PEG labels per particle based on band intensity is thus the only and best estimate of distribution of PEG labels.

For the second method, a double-labeling strategy was used. After attaching the PEG labels, P1 and P2 were then labeled on available Lys residues with a fluorescent dye, NHS-AlexaFluor647. Double-labeling has been found an effective method to determine the number of small chemical modifiers that are difficult to quantify by direct methods; for example, the number of biotin labels displayed on CPMV has been quantified using this method [17].

Using the double-labeling strategy, particles were first labeled with PEG, purified, and subsequently labeled with the fluorescent dye. Successful decoration of the samples with the AlexaFluor dyes was confirmed using UV/visible spectroscopy (Figure 2B) and native (Figure 1A) as well as denaturing gel electrophoresis (not shown). Dye-labeled particles have a higher mobility in native gels (Figure 1A, lane 4). The fact that the dye-modified P1 and P2 formulations also have an increased mobility in the gel towards the anode indicates successful double-labeling (Figure 1A, lane 5+6).

Quantitation of dyes per CPMV was carried out using UV/visible spectroscopy and the specific extinction coefficient for the AlexaFluor dye 647. The theoretical number of PEG molecules can be calculated by comparing the number of dyes per P1 or P2 to the amount of dyes found per native CPMV particles, the difference equals the theoretical number of PEG moieties per particle. Overall, it was found that fewer dyes were attached to P2 (16 ± 5) compared to P1 (27 ± 5), hence we conclude more PEG chains were attached to P2 (~ 38) versus P1 (~ 27). Additional methods to further quantify PEG attachment, such as barium iodode staining[16] or mass spectrometry, were attempted but the sensitivity was not sufficient to provide further quantitation (data not shown).

It was found, using either method, that more PEGs were attached per P2 particle compared to P1. When comparing the two methods used, it appears that quantitation of PEG polymers per CPMV using the double-labeling method overestimates the number of PEGs attached. Using

this method, it is assumed that every non-PEGylated Lys residue is accessible and thus available to undergo facile coupling with the fluorescent label. Our data indicate that this is not the case and that the PEG polymers are shielding the capsid surface, therefore preventing additional dyes from coupling with surface lysines. This hindrance is most likely be explained by an increased hydrodymanic radiues and hydration shell of the particles (see Figure 2C). Interestingly this shielding effect seems to be more effective for the P2 formulation. Here the theoretical number of PEG molecules, as determined by double-labeling method, overestimates the experimental value determined by band intensity method of about 40 %. For a comparison, the error for the P1 particles lies at only around 20 %. The differences might be attributed to the number of PEG chains attached or to the surface grafting area, however, differences in the number of labels comparing P1 and P2 were minor. Therefore it is more likely that the observed differences can be attributed to variations in effective surface area covered and/or the conformation in which the polymers are presented.

Shielding efficiency of P1 and P2 *in vitro* and *ex vivo*

We next investigated the shielding properties of the P1 and P2 formulations by asking whether PEGylation reduces or eliminates the interaction of CPMV with human tumor cells and tumor tissues. In previous studies it has been found that CPMV naturally interacts with endothelial cells, especially in tumor endothelium [5]. We tested several tumor cell lines and found using flow cytometry (Figure 3) and confocal microscopy (not shown) that native CPMV interacts strongly with HT-29 cells, a human colon adenocarcinoma cell line. To investigate the efficiency in inhibiting or reducing CPMV-cell interactions, binding assays were conducted on HT-29 cells *in vitro* and HT-29 tumor sections *ex vivo*.

Flow cytometry was used to compare CPMV, P1, and P2 binding and uptake studies on HT-29 cells and HT-29 tumor sections. To detect binding, cells were fixed prior to adding the different CPMV formulations. Detection was carried out using anti-CPMV antibodies followed by secondary dye-labeled antibodies. Prior to using anti-CPMV antibodies for flow cytometry or confocal microscopy, we have tested their ability to detect and bind CPMV, P1, and P2. ELISA studies confirmed that the antibodies detected PEGylated particles with the same efficiency as wild-type CPMV (see Supporting Information Figure S1). The low density of PEG-labeling (less than 30 PEG chains per particle) may explain why PEGylation does not impair detection using polyclonal anti-CPMV sera, while still affecting cell interaction. The portions of the CPMV capsid that interact with mammalian cells have not been identified yet. The data presented here suggest that regions in proximity to Lys 38 on S and Lys 99 on L may play an essential role; this are the areas shielded by the PEG chains (see below). The fact that PEGylation does not impair detection using polyclonal anti-CPMV sera raised in rabbit could be explained by the fact that the collection of CPMV-specific antibodies within the polyclonal serum may recognize a broader spectrum of CPMV surface epitopes than what is covered by PEGylation.

In order to study CPMV uptake, live cells were incubated with the different CPMV formulations, then fixed and permeabilized, followed by detection using antibodies (Figure 3). To study binding, cells were fixed prior to adding CPMV and staining using antibodies. The efficiency of native CPMV binding and uptake in HT-29 cells was about 20 %. Binding and uptake of P1 and P2 particles was reduced in both cases and most significantly for the P2 formulation. For P1 it was found that cell binding and uptake was reduced only about 55 % and 30 %, respectively, compared to native CPMV. For P2, a 90 % reduction in binding and an 80 % reduction in uptake was achieved.

Studying CPMV, P1, and P2 binding to HT-29 tumor sections *ex vivo* gave similar results. CPMV particles bound to the HT-29 tumor tissue sections, whereas binding of P1 was reduced

and no binding of P2 was observed (Figure 4). Overall, this is in good agreement with observations made during dye double-labeling studies and findings from *in vitro* assays.

Determining the PEG conformation based on PEG chains attached per CPMV

According to de Gennes, two conformational states have been identified for polymers grafted on surfaces, which are referred to as mushroom- and brush-conformation [18]. In the brush-like conformation the polymers are stretched out perpendicularly from the surface. In contrast, in the mushroom-like conformation the polymer is folded around the anchoring site into a more compact structure.

Considering the fact that PEG2000 is double the contour length (L_C) compared to PEG1000 it is expected that differences in particle size are dependent on the regime of PEG conformation. For example, if both PEG chains were presented in a brush conformation, one would expect the P2 formulation to be larger in diameter. On the other hand, smaller differences in particles size would be expected when presented in a mushroom-like conformation.

Differences in particle size were not apparent from TEM measurements, so DLS was performed. DLS studies showed that PEGylated particles have a significantly increased hydrodynamic radius compared to native CPMV ($p < 0.05$; Figure 2C). The findings are in good agreement with observations made by native gel electrophoresis, which also indicated an increase in size of PEGylated CPMV particles (Figure 1A). Differences between P1 and P2 were not significant, however, if anything the P2 formulation is slightly smaller. This implies that the PEG2000 is displayed in a more compact conformation compared to PEG1000 and suggests that the grafting surface area covered by the PEG polymer is greater on the P2 particle. This is in good agreement with findings from double-labeling experiments, which showed that the P2 formulation is more efficient in shielding the particle surface.

The conformation in which the PEG chains are displayed on the nanoparticles and the grafting density will determine the effective grafting surface area and thus the shielding efficiency. Several regimes of PEG surface conformation have been identified that are based on the grafting density. If the grafting density is low, the PEG chains are likely to be presented in a mushroom-like conformation; if the grafting density is high, the chains are stretched out and the PEG layer appears in a brush-like conformation. According to de Gennes the conformation can be estimated based on the distance (D) between two adjacent PEG chains relative to their Flory dimension (R_F), the latter being related to the chain length[3, 18–20]. A brush-like conformation appears when $D < R_F$, here the polymers stretch out perpendicularly from the surface. The polymer folds into a mushroom-like conformation when $D > R_F$ is given, and intermediate structures are observed at $D \sim R_F$ [18].

The Flory dimension is given by $R_F = aN^{3/5}$, where a is the persistence length of the PEG monomer (a = 3.5 Å) [20] and N the number of PEG monomers (N = 23 for PEG1000 and N = 45 for PEG2000) 18. The Flory dimension of the PEG polymers was calculated and is R_F PEG1000 = 22.8 Å and R_F PEG2000 = 34.5 Å, respectively.

The distance (D) between two adjacent PEG chain can be estimated using the atomic coordinates of CPMV. The structure of CPMV has been solved to near atomic resolution [15] and the atomic coordinates are available at http://viperdb.scripps.com (PDB file: 1NY7). The PEG molecules were attached to solvent-exposed Lys side chains on CPMV, less than every second subunit was modified with a PEG label. The chemistry and reactivity of solvent-exposed Lys residues on CPMV has been extensively studied[11,12]. It has been shown that Lys 38 on S and Lys 99 on L are the most reactive residues 11 (Figure 5). Denaturing protein gels (see Figure 1D) confirmed that both subunits (S and L) were labeled with PEG. We therefore make the assumption that the PEG labels are attached either Lys 38 on S or Lys 99 on L. Based on

quantitative analysis of band intensity in protein gels (see Figure 2A) we found that 22 ± 1 labels were displayed on P1 and 27 ± 4 per P2 particle. In both cases more labels were attached on L compared to S, with a ratio of L:S of 1.7 and 1.8 for P1 and P2, respectively.

To determine the average distance (D) between adjacent PEG labels we made the following assumptions: i) the labels are evenly distributed over the whole particle surface, ii) alternating Lys 38 on S and Lys 99 on L are modified, whereby nearly two times as many Lys 99 are labeled, and iii) the possibility that two neighboring Lys residues (D ~ 15 Å, Figure 3) are labeled will not be taken into account. Based on these assumptions, the average distance was determined to be around 70 Å (Figure 5). With regard to the Flory dimension (see above) it is implied that both PEG chains, PEG1000 and PEG2000, are presented as separate mushrooms on the viral capsid surface.

Assuming a fully PEGylated CPMV formulation, that is CPMV displaying 300 PEG labels (either PEG1000 or PEG2000), in this case the PEG labels are still likely to be presented as mushrooms. However, the potential exists that some PEG chains are presented as brushes; this could be the case for neighboring labeled Lys 38 on S and Lys 99 residues (Figure 5a).

Presentation of PEG labels in the mushroom conformation is in good agreement with findings from DLS measurements (Figure 2C). If the PEG chains would be presented in a stretched form, i.e. brush-like orientation, a large increase of the hydrodynamic radii of P1 and P2 would be expected (Figure 5B); the contour length of the polymers is LC PEG1000 = 80.5 Å and LC PEG2000 = 157.5 Å. Using DLS it was found that P1 and P2 have an increased radius (see Figure 2C), however, increase was only of about 14 Å and 10 Å for P1 and P2 with regard to native CPMV. This is in good agreement with PEG chain being presented in a mushroom-like orientation. The fact that the increase in radius as determined by DLS is lower than one would expect looking at the Flory dimension of the polymers with R_F PEG1000 = 22.8 Å and R_F PEG2000 = 34.5 Å, respectively, can be explained by the fact that the PEG chains are attached in a depression on the particle surface (see location of Lys 38 on S and Lys 99 on L; Figure 5A).

Estimating the surface grafting area of the P1 and P2 formulations in relation to shielding efficiency

The theoretical surface area (Γ) occupied by a single PEG molecule can be calculated based on the molecular weight (MW), its density (ρ = 1.1 g cm^{-3}) and height (h = R_F) using the following equation: Γ = MW/(ρ*h*N_A) with NA = Avogadro's constant[21]. The area covered by the PEG chains is Γ PEG1000 = 66.4 Å2 and Γ PEG2000 = 87.4 Å2. The total coverage area can be estimated taken the total number of labels into account, which gives Γ total PEG1000 = 1486.2 Å2 and Γ total PEG2000 = 2325.1 $Å^2$. That means that about 0.53 % (P1) and 0.83 % (P2) of the total surface area of CPMV are effectively covered with PEG chains (calculations are based on the estimation that CPMV is a sphere with an average radius of 15 nm). Of course, one must take into account that the flexible PEG chains potentially rotate around the attachment site on the virion and thus could occupy and block the surface area round that radius. Nevertheless, the surface area occupied by PEG on P1 or P2 is extremely small relative to the total surface area.

It is remarkable that little biochemical and biophysical differences between P1 and P2 have significant input on the biological properties and shielding efficiency. It appears that we detected the threshold of PEGylation required to achieve sufficient blocking and effective shielding from CPMV-cell interactions. Effective shielding was only achieved for P2.

In previous reports it has been found that the natural CPMV-cell interactions can be blocked using either 30 copies of PEG3400 or PEG5000, or by attachment of 60 copies of PEG500[5,

[7,8]. An issue when working with high molecular weight PEG molecules is aggregation or precipitation of the viral nanoparticles upon storage. This has not been observed for the P2 formulation, which was monitored over a time frame of about three months.

It is interesting that attaching less than 30 copies of PEG1000 did not yield effective shielding, but decorating CPMV with 60 PEG500 moieties was sufficient to block CPMV-cell interactions [7]. In 27 the latter example, both subunits were labeled with PEG500 chains; with a Flory dimension of $R_F = 4.2$ (N = 11) the PEG500 chains were also presented as compact mushrooms. The surface coverage area shielded by PEG500 on CPMV lies at Γ total PEG500 = 3070.2 $Å^2$ (based on the Flory dimension), which accounts for 1.1 % of the total CPMV capsid surface. Thus although the PEG500 chains are shorter, it appears that as long as the PEG chains are attached to every single subunit, sufficient coverage results such that effective shielding can be achieved.

In general, the shielding effect of PEG can be explained by i) steric repulsion due to the polymer chain or ii) repulsion based on the presence of the hydration shell of the polymers[22]. The fact that covering only a small fraction of the particle surface with PEG chains allows effective shielding of cell interactions, may suggest that coverage of the CPMV key surface areas that are necessary for cellular interactions was achieved; this is true for P2 but not for P1 particles. The mammalian CPMV cell surface receptor has been identified as a 54 kDa non-glycosylated cell surface protein [6]. It is not known which capsid surface regions specifically bind to the 54 kDa protein. The data presented here imply that in the P2 formulation key epitopes were effectively shielded, thus it is possible that key areas lie in near proximity to Lys 38 on S and Lys 99 on L. An alternative possibility is that a sufficient hydration shell is generated with a broader distribution of P500 or narrower distribution of P2000. Future studies could include installing the PEG chains at different positions, to verify that indeed the attachment site is key factor, but also to analyze the impact of conjugation chemistry on surface charge. For example, PEG chains could be attached to solvent exposed carboxylates or tyrosines on CPMV. Once the key surface areas have been identified, future experiments could also include mutagenesis studies to identify CPMV epitopes that interact with mammalian receptors. The potential exists to make use of genetic engineering in order to design CPMV chimeras that are essentially non-interacting with cells. As an example, genetically modifying key epitopes of adeno-associated virus, a promising vector for gene therapy, yielded particles that were effectively “shielded” and could evade serum neutralization [23, 24].

The finding that only a small fraction of the CPMV particle needs to be covered with PEG chains in order to achieve efficient blocking of CPMV-cell interactions is intriguing. This means that a large surface area of the particles remains available for further display of either targeting and/or imaging molecules. For targeted formulations it would be important for the targeting molecule to have access to the surroundings and not be completely covered by PEG. The potential exists to either genetically introduce targeting ligands into the capsid or to attach them chemically. For a genetic approach, the so-called βB-βC loop within the S protein would almost be ideal for display of targeting molecules, as it is extremely solvent-exposed, not in near proximity to Lys 38 on S and Lys 99 on L, and is permissive for genetic engineering [25–27]. Various chemical modification approaches are available as well, for example further Lys residues can be modified [11] as we have shown, or alternatively solvent-exposed carboxylates could be utilized [28]. In addition, by using a bivalent PEG, further moieties could be displayed at the termini of the PEG chains.

Conclusions

PEGylation is known to be an effective strategy in biomedical research and is widely used to reduce non-specific and specific interactions between biomolecules or nanoparticles and cells

and tissues *in vitro* and *in vivo*. We found that PEGylating CPMV is indeed an effective strategy to reduce or eliminate interactions of CPMV with mammalian tumor cells and tumor tissues. However, the degree of reduced interaction is strongly dependent on the particle formulation. Particles decorated with PEG2000 (P2) could effectively block interactions of CPMV nanoparticles with cells and tumor tissue sections; binding was reduced of about 80–90 % in cells and no binding was observed studying tumor tissue sections. In stark contrast was the ability of P1 particles (i.e. CPMV decorated with PEG1000) to block binding to mammalian cells or tissue sections; in this case shielding efficiency was only around 30–55 %.

A variety of factors impact the degree of shielding efficiency, including the number of PEG chains displayed, the density in which the PEG is displayed, its molecular weight, its conformation, and location [2]. In this study, the number of PEG chains attached was not significantly different: 22 ± 1 versus 27 ± 4 were attached per P1 and P2, respectively. The surface grafting area on CPMV that is effectively shielded by the PEG chains was found to be 0.53 % for the P1 formulation and 0.83 % for P2. Thus the grafting area that is effectively shielded by the PEG polymers is extremely small compared to the overall surface area of CPMV. Striking also is the fact that subtle differences in percent surface coverage (P1 versus P2) have a significant impact on the biological properties of the particles.

The requirements for effective shielding have been addressed using various nanomaterial systems, including dendrimers, liposomes, and adenovirus vectors. Overall, it has been shown that the more PEG ligands and the higher the molecular weight of the PEG attached, the more efficiently the particles are shielded [29–31]. However, when aiming for multifunctional devices it is important to find the minimal requirements needed to achieve shielding. It appears that with the attachment of < 30 PEG labels to solvent-exposed Lys residues effective shielding can be accomplished when using PEG2000. This not only allows further engineering of the particle surface using either genetic modification or chemical bioconjugation, moreover this suggests that the key areas participating in CPMV-cell interactions have been blocked. For future development of targeting devices based on CPMV for imaging or therapy we will use design principles based on the P2 formulation. Studies to this end are in progress in our laboratory.

Supplementary Material

Refer to Web version on PubMed Central for supplementary material.

Acknowledgments

Dr. Giuseppe Destito and Dr. Rebecca Taurog are thanked for help with TEM studies. Prof. M.G. Finn is thanked for providing the DLS instrument. This study was funded by NIH grant CA112075 to M.M., and an American Heart Association Postdoctoral Fellowship to N.F.S.

References

1. Harris JM, Chess RB. Effect of pegylation on pharmaceuticals. Nat Rev Drug Discov 2003;2(3):214–221. [PubMed: 12612647]
2. Roberts MJ, Bentley MD, Harris JM. Chemistry for peptide and protein PEGylation. Adv Drug Deliv Rev 2002;54(4):459–476. [PubMed: 12052709]
3. Wattendorf U, Merkle HP. PEGylation as a tool for the biomedical engineering of surface modified microparticles. J Pharm Sci. 2008
4. Steinmetz, NF. Plant viral capsids as programmable nanobuilding blocks. In: Pignataro, B., editor. Tomorrow's Chemistry Today. WILEY-VCH Verlag GmbH & Co. KGaA; 2008. p. 215-237.

5. Lewis JD, Destito G, Zijlstra A, Gonzalez MJ, Quigley JP, Manchester M, Stuhlmann H. Viral nanoparticles as tools for intravital vascular imaging. Nat Med 2006;12(3):354–360. [PubMed: 16501571]
6. Koudelka KJ, Rae CS, Gonzalez MJ, Manchester M. Interaction between a 54-kilodalton mammalian cell surface protein and cowpea mosaic virus. J Virol 2007;81(4):1632–1640. [PubMed: 17121801]
7. Destito G, Yeh R, Rae CS, Finn MG, Manchester M. Folic acid-mediated targeting of cowpea mosaic virus particles to tumor cells. Chem Biol 2007;14(10):1152–1162. [PubMed: 17961827]
8. Raja KS, Wang Q, Gonzalez MJ, Manchester M, Johnson JE, Finn MG. Hybrid virus-polymer materials. 1. Synthesis and properties of PEG-decorated cowpea mosaic virus. Biomacromolecules 2003;3:472–476. [PubMed: 12741758]
9. Bruckman MA, Kaur G, Lee LA, Xie F, Sepulveda J, Breitenkamp R, Zhang X, Joralemon M, Russell TP, Emrick T, Wang Q. Surface modification of tobacco mosaic virus with “click” chemistry. Chembiochem 2008;9(4):519–523. [PubMed: 18213566]
10. Schlick TL, Ding Z, Kovacs EW, Francis MB. Dual-surface modification of the tobacco mosaic virus. J Am Chem Soc 2005;127:3718–3723. [PubMed: 15771505]
11. Chatterji A, Ochoa W, Paine M, Ratna BR, Johnson JE, Lin T. New addresses on an addressable virus nanoblock: uniquely reactive Lys residues on cowpea mosaic virus. Chem Biol 2004;11(6):855–863. [PubMed: 15217618]
12. Wang Q, Kaltgrad E, Lin T, Johnson JE, Finn MG. Natural supramolecular building blocks: Wild-type cowpea mosaic virus. Chem Biol 2002;9(7):805–811. [PubMed: 12144924]
13. Wellink J. Comovirus isolation and RNA extraction. Meth Mol Biol 1998;81:205–209.
14. Steinmetz NF, Evans DJ, Lomonossoff GP. Chemical introduction of reactive thiols into a viral nanoscaffold: a method that avoids virus aggregation. Chembiochem 2007;8(10):1131–1136. [PubMed: 17526061]
15. Lin T, Chen Z, Usha R, Stauffacher CV, Dai JB, Schmidt T, Johnson JE. The refined crystal structure of cowpea mosaic virus at 2.8 A resolution. Virology 1999;265(1):20–34. [PubMed: 10603314]
16. Kurfurst MM. Detection and molecular weight determination of polyethylene glycol-modified hirudin by staining after sodium dodecyl sulfate-polyacrylamide gel electrophoresis. Anal Biochem 1992;200(2):244–248. [PubMed: 1378701]
17. Steinmetz NF, Calder G, Lomonossoff GP, Evans DJ. Plant viral capsids as nanobuilding blocks: construction of arrays on solid supports. Langmuir 2006;22(24):10032–10037. [PubMed: 17106996]
18. de Gennes PG. Polymers at an interface: a simplified view. Adv Colloid Interface Sci 1987;27:189–209.
19. Nicholas AR, Scott MJ, Kennedy NI, Jones MN. Effect of grafted polyethylene glycol (PEG) on the size, encapsulation efficiency and permeability of vesicles. Biochim Biophys Acta 2000;1463(1): 167–178. [PubMed: 10631306]
20. Svergun DI, Ekstrom F, Vandegriff KD, Malavalli A, Baker DA, Nilsson C, Winslow RM. Solution structure of poly(ethylene) glycol-conjugated hemoglobin revealed by small-angle X-ray scattering: implications for a new oxygen therapeutic. Biophys J 2008;94(1):173–181. [PubMed: 17827244]
21. Zhu B, Eurell T, Gunawan R, Leckband D. Chain-length dependence of the protein and cell resistance of oligo(ethylene glycol)-terminated self-assembled monolayers on gold. J Biomed Mater Res 2001;56(3):406–416. [PubMed: 11372059]
22. Lee GK, Maheshri N, Kaspar B, Schaffer DV. PEG conjugation moderately protects adeno-associated viral vectors against antibody neutralization. Biotechnol Bioeng 2005;92(1):24–34. [PubMed: 15937953]
23. Huttner NA, Girod A, Perabo L, Edbauer D, Kleinschmidt JA, Buning H, Hallek M. Genetic modifications of the adeno-associated virus type 2 capsid reduce the affinity and the neutralizing effects of human serum antibodies. Gene Ther 2003;10(26):2139–2147. [PubMed: 14625569]
24. Wu P, Xiao W, Conlon T, Hughes J, Agbandje-McKenna M, Ferkol T, Flotte T, Muzyczka N. Mutational analysis of the adeno-associated virus type 2 (AAV2) capsid gene and construction of AAV2 vectors with altered tropism. J Virol 2000;74(18):8635–8647. [PubMed: 10954565]
25. Porta C, Spall VE, Findlay KC, Gergerich RC, Farrance CE, Lomonossoff GP. Cowpea mosaic virus-based chimaeras. Effects of inserted peptides on the phenotype, host range, and transmissibility of the modified viruses. Virology 2003;310(1):50–63. [PubMed: 12788630]

26. Porta C, Spall VE, Lin T, Johnson JE, Lomonossoff GP. The development of cowpea mosaic virus as a potential source of novel vaccines. Intervirology 1996;39(1–2):79–84. [PubMed: 8957673]

27. Porta C, Spall VE, Loveland J, Johnson JE, Barker PJ, Lomonossoff GP. Development of cowpea mosaic virus as a high-yielding system for the presentation of foreign peptides. Virology 1994;202 (2):949–955. [PubMed: 8030255]

28. Steinmetz NF, Lomonossoff GP, Evans DJ. Cowpea mosaic virus for material fabrication: addressable carboxylate groups on a programmable nanoscaffold. Langmuir 2006;22(8):3488–3490. [PubMed: 16584217]

29. Wortmann A, Vohringer S, Engler T, Corjon S, Schirmbeck R, Reimann J, Kochanek S, Kreppel F. Fully detargeted polyethylene glycol-coated adenovirus vectors are potent genetic vaccines and escape from pre-existing anti-adenovirus antibodies. Mol Ther 2008;16(1):154–162. [PubMed: 17848961]

30. Okuda T, Kawakami S, Akimoto N, Niidome T, Yamashita F, Hashida M. PEGylated lysine dendrimers for tumor-selective targeting after intravenous injection in tumor-bearing mice. J Control Release 2006;116(3):330–336. [PubMed: 17118476]

31. Kaminskas LM, Boyd BJ, Karellas P, Krippner GY, Lessene R, Kelly B, Porter CJ. The Impact of Molecular Weight and PEG Chain Length on the Systemic Pharmacokinetics of PEGylated Poly l-Lysine Dendrimers. Mol Pharm 2008;5(3):449–463. [PubMed: 18393438]

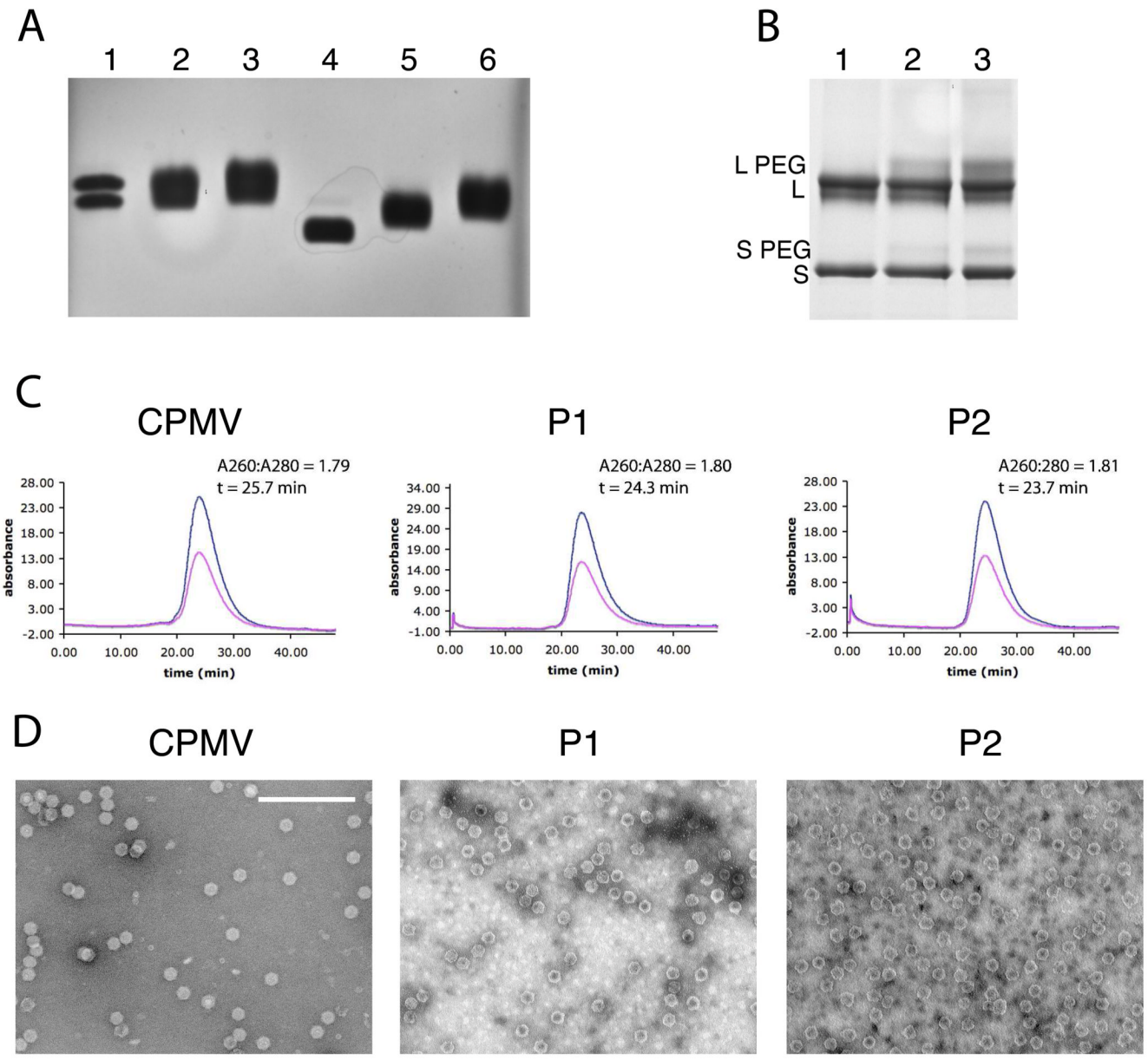

Figure 1. Structural integrity of PEGylated *Cowpea mosaic virus* (CPMV) particles

A+B: Gel electrophoresis separation of intact particles in a 1.2 % (w/v) agarose gel (A) and separation of the coat protein subunits using denaturing conditions and a 4–12 % NuPage gel (B). The small subunit (S) and the large subunit (L), are detectable as well as the chemically modified forms S-PEG and L-PEG, respectively. Both gels were stained using Coomassie blue. 1 = CPMV, 2 = P1 (CPMV-PEG1000), 3 = P2 (CPMV-PEG2000), 4 = CPMV-AF647 (CPMV labeled with AlexaFluor dye 647), 5 = P1-AF647, 6 = P2-AF647. (C). Size exclusion chromatography of native and PEGylated CPMV particles using a Sepharose6 column. Shown is the absorbance versus elution time. CPMV was followed at an absorbance of 260 nm to detect the encapsidated RNA (in blue) and at 280 nm detecting the protein coat (in pink). Inset: Elution time (t in min) as well as the absorbance ration of 260:280 nm is given. (D). Transmission electron microcrographs of CPMV, P1 and P2. Particles were negatively stained

using 2 % (w/v) uranyl acetate. The scale bar is 200 nm. The magnification was 73 K for all samples.

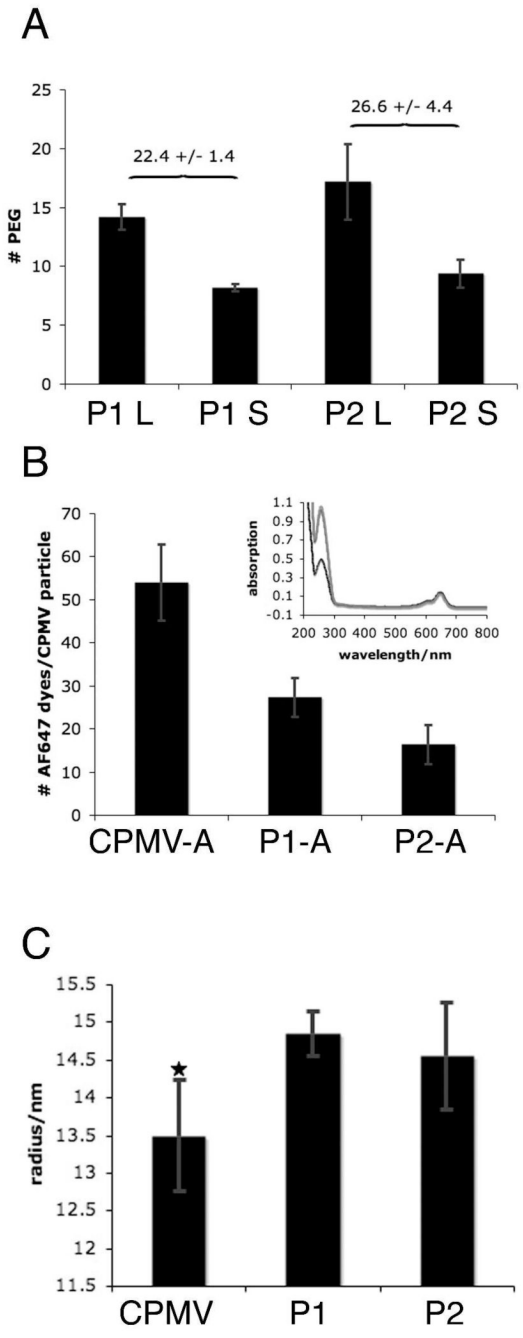

Figure 2. Biochemical characterization of PEGylated and AlexaFluor647-labeled *Cowpea mosaic virus* (CPMV) particles

A. Quantification of PEG labels per subunit of P1 and P2 (P1 = CPMV-PEG1000, P2 = CPMV-PEG2000) probes based on the band intensity of non-modified and PEGylated coat protein subunit bands after electrophoretic separation in denaturing gels. Five samples P1 and P2 each were analyzed, the band intensity of S versus S-PEG and L versus L-PEG, respectively, was compared using FluorChemSP software. The number of PEG (average and standard deviation) per subunit is shown. Statistical analysis of differences between S of P1 and P2 and L of P1 and P2 was performed using Student 2-tailed T-test (Microsoft Excel) where $P < 0.05$. B. Quantification of number of dyes per CPMV formulation (CPMV, P1, and P2) based on UV/

visible spectroscopy (see inset). The number was calculated using the respective extinction coefficients for CPMV and the AF647 dye. The number of AF647 (average and standard deviation) per CPMV particle is shown. C. Radii of CPMV, P1, and P2 particles determined by dynamic light scattering. Shown is the averaged radius (and standard deviation) for CPMV, P1, and P2 particles. Five measurements each were performed; each single measurement presents an average of ten measurements. Statistical analysis of differences between CPMV versus P1 and P2, respectively, was performed using Student 2-tailed T-test (Microsoft Excel), where * = $P < 0.05$.

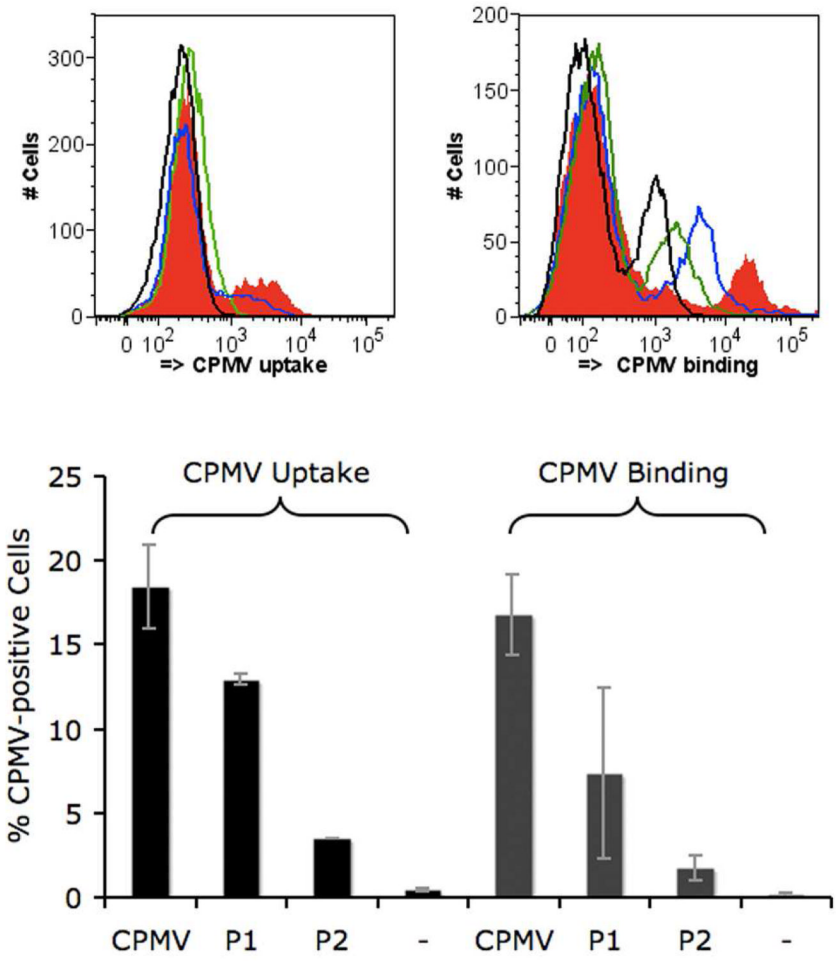

Figure 3. Interaction of native *Cowpea mosaic virus* (CPMV), P1 and P2 particles with HT-29 cells *in vitro* studied by flow cytometry

For uptake studies HT-29 cells were probed with CPMV and P1 and P2 formulations. P1 = CPMV-PEG1000, P2 = CPMV-PEG2000. Detection was carried out using anti-CPMV specific antibodies and AlexaFluor 647-conjugated secondary antibodies. Cells were also probed with antibodies only. Top panel: Histograms showing CPMV uptake (left) and binding (right). Red filled histogram = CPMV, blue histogram = P1, green histogram = P2, black histogram = antibodies only. Experiments were repeated at least twice and triplicate samples were analyzed. At least 10000 events gated for live cells were recorded. Bottom panel: Statistical analysis of the data using FlowJo software. The amount of CPMV-positive cells in % of total cells is shown for each case studied. Error bars indicate mean +/− S.D.

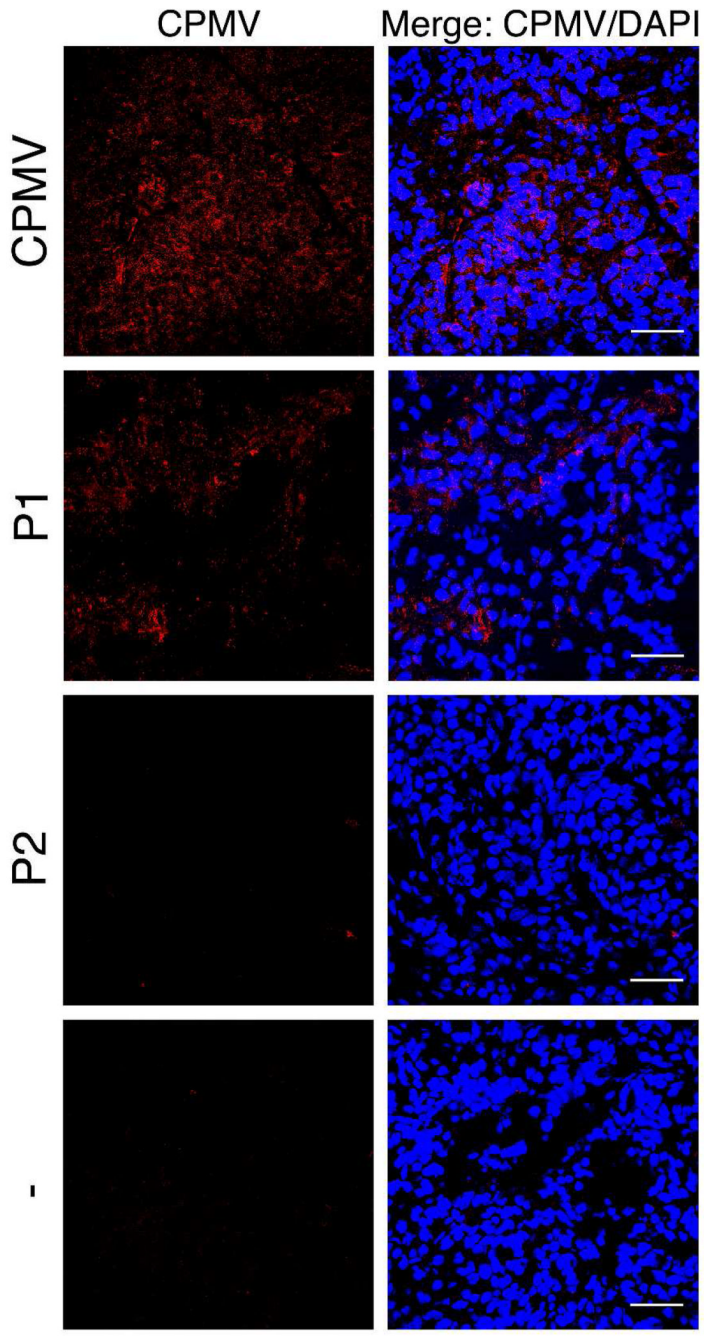

Figure 4. Interaction of native *Cowpea mosaic virus* (CPMV), P1 and P2 particles with HT-29 tumor sections *ex vivo* as studied by confocal microscopy

HT-29 tumor cryosections (10 μm thick) were fixed prior to probing with CPMV and different PEGylated CPMV particle formulations (P1 and P2). P1 = CPMV decorated with PEG MW 1000 Da, P2 = CPMV decorated with PEG MW 2000 Da. Detection was carried out using anti-CPMV specific antibodies and AlexaFluor 647-conjugated secondary antibodies. Tissues were also probed with antibodies only (bottom panel). Nuclei were stained with DAPI and are shown in blue. CPMV is shown in red. The scale bar is 50 μm.

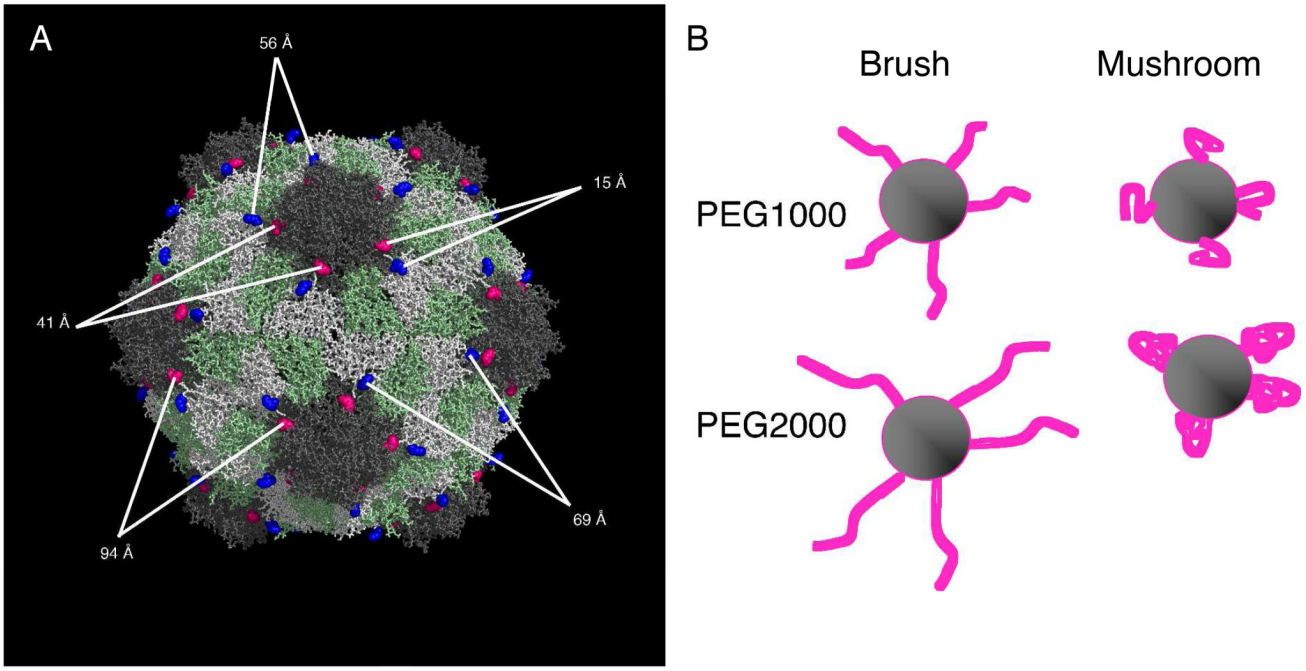

Figure 5. Structure of *Cowpea mosaic virus* (CPMV) and location of addressable surface lysine residues and cartoon showing possible PEG conformations

A. The small subunit (S) is shown in grey, the two domains of the large subunit (L) shown in white and green. Solvent-exposed addressable Lys residues Lys 38 on S and Lys 99 on L are highlighted as pink and blue sphere, respectively. The distances between pairs of Lys residues are indicated; measurements were determined using Pymol software. B. Cartoon showing PEG chains in a brush versus mushroom conformation. CPMV is shown as a grey sphere, PEG is depicted in pink.